

A CASPT2 Investigation of the Ground and First Excited Singlet States of Fluoroiodocarbene

Jean M. Standard*[†] and Robert W. Quandt*[‡]

Department of Chemistry, Illinois State University, Normal, Illinois 61790-4160

Received: April 24, 2003; In Final Form: June 13, 2003

The $\tilde{X}(^1A')$ and $\tilde{A}(^1A'')$ electronic states of CFI have been investigated using the CASPT2(18,12) method. Results for the ground-state equilibrium geometry of CFI are in excellent agreement with previous studies. The equilibrium geometry of the excited state shows significant variations in the C–I bond length as a function of basis set in part due to the flatness of the potential energy surface in the region of the minimum. The $\tilde{A}(^1A'') \leftarrow \tilde{X}(^1A')$ adiabatic transition energy for CFI is estimated to be in the range 17000–17500 cm^{-1} . A barrier in the exit channel for dissociation to CF + I was located on the excited-state surface, and the barrier height is predicted to be greater than 1525 cm^{-1} .

1. Introduction

Dihalocarbenes, in particular those containing fluorine, have received recent attention due to their importance as possible photoproducts from the atmospheric degradation of chlorofluorocarbons and hydrochlorofluorocarbons. For example, a number of recent experimental and theoretical studies have focused on the carbenes CFCl^{1-3} and $\text{CFBr}^{4,5}$.

While the parent carbene, CH_2 , long has been known to possess a triplet ground state, halocarbenes such as CFCl and CFBr have been predicted from molecular orbital arguments to possess singlet ground states⁶ and experimental studies have verified this prediction.^{1,2,4,5} Electronic transitions from the ground $\tilde{X}(^1A')$ state to the first excited singlet state, $\tilde{A}(^1A'')$, have been observed experimentally in the visible region, and spectroscopic information including vibrational constants have been obtained for both CFCl^{1-3} and $\text{CFBr}^{4,5}$.

To date, little experimental or computational data is available for the next carbene in the series, fluoroiodocarbene, CFI. Hajgato et al.⁷ and Schwartz and Marshall⁸ have reported ab initio results for the equilibrium geometry of the singlet ground electronic state of CFI and other halocarbenes, and in addition they have carried out extensive studies of triplet–singlet gaps of halocarbenes. The geometry optimizations were carried out at the $\text{CCSD(T)/6-311++G(d,p)}^7$ and QCISD/6-311G(d,p) levels,⁸ respectively. Both these studies accounted for any relativistic effects on the geometry of CFI by using effective core potentials to represent the core electrons of iodine. The studies also focused on the triplet–singlet gaps of halocarbenes including CFI. The calculated triplet–singlet gap of CFI was determined to be relatively large, ranging from 95 to 123 kJ/mol (7940–10280 cm^{-1}) depending on the level of theory and basis set. Hajgato and co-workers⁷ report that the CASPT2 method slightly underestimates the energy of the triplet state, leading to a somewhat lower triplet–singlet gap by about 15–20 kJ/mol (or about 15%) than that calculated by other methods.

Recently, the ground and first excited singlet states of a series of bromine- and iodine-containing carbenes were investigated

using CASSCF and CASPT2 methods.⁹ The calculations utilized effective core potentials along with a valence-only basis set of double- ζ quality augmented with d-type polarization functions. On the basis of comparisons with available experimental data, it was found that the CASPT2 method including 18 electrons in 12 active orbitals, denoted CASPT2(18,12), was successful in accurately predicting equilibrium geometries for the ground and first excited electronic singlet states of bromo- and iodocarbenes as well as adiabatic transition energies for $\tilde{A}(^1A'') \leftarrow \tilde{X}(^1A')$ transitions. In particular, at the CASPT2(18,12) level, the singlet–singlet gap for CHBr was calculated to be 11712 cm^{-1} compared to the experimental result of 11972 cm^{-1} ; for CFBr , the calculated value was 21369 cm^{-1} compared to the experimental result of 20906 cm^{-1} ; and for CBr_2 , the calculated singlet–singlet gap was 15192 cm^{-1} relative to experimental values of 14885 and 15093 cm^{-1} .⁹

In the previous study,⁹ some unusual convergence behavior was observed for the fluorocarbenes CFBr and CFI . An equilibrium geometry corresponding to a minimum on the excited state potential energy surface could be located only at the highest level of theory employed, CASPT2(18,12), for both CFBr and CFI . Other recent computational work on CFBr at the CASPT2(18,12) level,⁴ carried out using the all-electron cc-pVTZ basis set, indicates that the potential well on the $\tilde{A}(^1A'')$ surface is rather shallow and is very sensitive to the level of electron correlation employed in the calculations. A barrier height for dissociation to $\text{CF} + \text{Br}$ of 3455 cm^{-1} was determined at the CASPT2 level. The situation for the first excited singlet state of CFCl is similar to that for CFBr ; however, the barrier height is larger, determined by the CASPT2 method to be 5699 cm^{-1} .³

The $\tilde{A}(^1A'') \leftarrow \tilde{X}(^1A')$ transition of CFI has not yet been detected experimentally. For halocarbenes such as CCl_2 and CBr_2 , the excited-state inversion barrier is predicted to be less than the dissociation energy.¹⁰ This leads to Renner–Teller coupling between the excited and ground states, which greatly enhances the odds of a nonradiative transition back to the ground state. This effect explains the weak emission seen by Clouthier and co-workers in studies of CFCl and CCl_2 .¹¹ For these cases, a direct absorption measurement is preferable, but often not practical, due to low sensitivity. One solution is the use of a

* Corresponding authors.

[†] E-mail: standard@ilstu.edu.

[‡] E-mail: quandt@xenon.che.ilstu.edu.

TABLE 1: Equilibrium Geometry of the Ground $\tilde{X}(^1A')$ State of CFI Calculated at the CASPT2(18,12) Level Using Various Basis Sets^a

	CASPT2(18,12)/ SBKJC(3d) ^a	CASPT2(18,12)/ SBKJC(3df) ^b	CASPT2(18,12)/ Basis3 ^b	CCSD(T)/ 6-311+G(d,p) ^c	QCISD/ 6-311G(d,p) ^d
C–F distance (Å)	1.313	1.306	1.306	1.296	1.290
C–I distance (Å)	2.217	2.208	2.218	2.193	2.189
F–C–I angle (deg)	107.6	107.0	106.9	107.4	107.4

^a Previous literature results are included for comparison. ^b Drake, Standard, and Quandt.⁹ ^c This work. ^d Hajgato and co-workers.⁷ ^e Schwartz and Marshall.⁸

novel multipass absorption method termed cavity ringdown laser absorption spectroscopy, CRDLAS.¹² The effectiveness of CRDLAS in detecting low concentration transient species has been recently demonstrated.¹³ The main advantage of CRDLAS is that in addition to being highly sensitive it is an absorption technique, so it is applicable to systems with poorly behaved upper states such as some halocarbenes. However, since the highly reflective dielectric mirrors used for CRDLAS are expensive and have a limited spectral width (~50 nm), they must be chosen carefully for the particular system under study.

To further understand the unusual convergence behavior of the first excited singlet state of CFI and to make predictions for experimental detection of the $\tilde{A}(^1A'') \leftarrow \tilde{X}(^1A')$ transition of CFI, ab initio calculations of the ground and first excited singlet states of CFI employing the CASPT2 method with a variety of basis sets have been performed. Results are reported for equilibrium geometries of the ground and excited states, along with a more detailed investigation of the excited-state potential energy surface. In addition, adiabatic transition energies for the $\tilde{A}(^1A'') \leftarrow \tilde{X}(^1A')$ transition are reported.

2. Methods

In our previous study of CFI,⁹ it was found that the CASSCF method was not adequate for determining the equilibrium geometry of the first excited singlet state. Using the CASSCF method, no minimum was located on the potential energy surface. Therefore, in this work calculations on the ground and first excited singlet states of CFI were performed using the CASPT2 method. A full valence active space was utilized which included 18 valence electrons and 12 active orbitals; these calculations are referred to as CASPT2(18,12). The software package MOLPRO¹⁴ was employed for all the studies. Computations were carried out using an SGI Origin2000 computer at the National Center for Supercomputing Applications in Urbana, IL, along with SGI O2 and Linux workstations at Illinois State University.

To study basis set effects on the geometries and energies of CFI, three basis sets were utilized. The calculations employed the Stevens, Basch, Krauss, Jasien, and Cundari (SBKJC) relativistic effective core potentials along with the corresponding valence-only basis sets of double- ζ quality.^{15–17} The first basis set was constructed by augmenting the SBKJC basis with three sets of d-type polarization functions on each atom. This basis set, henceforth referred to as SBKJC(3d), was employed in our previous study.⁹ The second basis set was constructed by further augmenting the SBKJC(3d) basis with a set of f-type polarization functions on each atom, and will be referred to as SBKJC(3df). Finally, a third basis set was constructed by using the SBKJC effective core potential and the SBKJC(3df) basis for iodine along with an all-electron double- ζ basis for carbon and fluorine augmented with three sets of d-type and one set of f-type polarization functions, DZ(3df); this basis set will be referred to as Basis3.

Full optimizations of the geometries of the ground $\tilde{X}(^1A')$ and excited $\tilde{A}(^1A'')$ states of CFI were carried out using the

CASPT2(18,12) method with the three different basis sets. A transition state in the exit channel for dissociation to CF + I was also located on the $\tilde{A}(^1A'')$ potential energy surface. The convergence criteria for the equilibrium geometry and transition state optimizations were 3×10^{-4} for the RMS gradient and 5×10^{-4} for the maximum component of the gradient. Because of its interesting features, potential surface scans of the $\tilde{A}(^1A'')$ state of CFI were carried out in order to further characterize the potential energy surface.

3. Results and Discussion

A. Ground-State Results. Results for the equilibrium geometry of the ground $\tilde{X}(^1A')$ state of CFI are reported in Table 1. While no experimental data exists for the ground state of CFI, previous computational results are included for comparison.^{7–9}

The present results for the ground-state equilibrium geometry of CFI are in good agreement with previous ab initio results. The calculated C–F bond distance is 1.306 Å from the SBKJC(3df) and Basis3 basis sets compared to the literature values of 1.296⁷ and 1.290 Å.⁸ In addition, the present results obtain F–C–I bond angles of 107.0 and 106.9° from the SBKJC(3df) and Basis3 basis sets, respectively, compared to the literature results of 107.4°.^{7,8} Values of the C–I bond distance calculated in this study are 2.208 and 2.218 Å from the SBKJC(3df) and Basis3 basis sets, respectively, while previous literature studies obtained 2.193⁷ and 2.189 Å.⁸ Overall, the results from the SBKJC(3df) basis set are in the best agreement with the previous literature studies. Deviations of only 0.010 Å for the C–F bond, 0.015 Å for the C–I bond, and -0.4° for the F–C–I angle are obtained when the present results are compared with the results of Hajgato et al.⁷ When the present results from the SBKJC(3df) basis set are compared with those of Schwartz et al.,⁸ deviations of 0.016 Å for the C–F bond, 0.019 Å for the C–I bond, and -0.4° for the F–C–I angle are obtained.

The effects of the addition of f-type polarization functions to the basis set can be observed by comparison of the present results with the SBKJC(3df) basis to the previous work carried out with the SBKJC(3d) basis.⁹ The C–F and C–I bonds are shortened by 0.007 and 0.009 Å, respectively, while the F–C–I bond angle decreases by 0.6° when f-type polarization functions are added to the basis set. The use of f-type polarization functions brings the bond lengths into closer agreement with the previous literature studies.^{7,8}

The use of all-electron basis sets on carbon and fluorine in Basis3 has only a small effect on the equilibrium geometry of the ground state of CFI. Results from calculations with the all-electron DZ(3df) basis set for carbon and fluorine in Basis3 produces a C–F bond with the same length, a slightly longer C–I bond by 0.010 Å, and a slightly smaller F–C–I angle by 0.1° compared to the results obtained with the SBKJC(3df) basis set. The similar results obtained for the SBKJC(3df) and Basis3 basis sets are not surprising since the only significant difference between the basis sets is the use of a double- ζ basis set to

TABLE 2: Equilibrium Geometry of the First Singlet Excited $\tilde{A}(^1A'')$ State of CFI Calculated at the CASPT2(18,12) Level Using Various Basis Sets^a

	CASPT2(18,12)/SBKJC(3d) ^a	CASPT2(18,12)/SBKJC(3df) ^b	CASPT2(18,12)/Basis3 ^b
C–F distance (Å)	1.308	1.310	1.303
C–I distance (Å)	2.426	2.165	2.130
F–C–I angle (deg)	121.7	124.8	125.8

^a Previous literature results are included for comparison. ^b Drake, Standard, and Quandt.⁹ ^c This work.

TABLE 3: Electronic Energies of the $\tilde{X}(^1A')$ and $\tilde{A}(^1A'')$ States and Adiabatic Transition Energies (T_e) for the $\tilde{A}(^1A'') \leftarrow \tilde{X}(^1A')$ Transition of CFI Calculated at the CASPT2(18,12) Level Using Various Basis Sets^a

	CASPT2(18,12)/SBKJC(3d) ^a	CASPT2(18,12)/SBKJC(3df) ^b	CASPT2(18,12)/Basis3 ^b
$\tilde{X}(^1A')$ energy (au)	−40.915530	−40.984123	−148.958016
$\tilde{A}(^1A'')$ energy (au)	−40.835759	−40.906850	−148.884037
T_e (cm ^{−1})	17 508	16 959	16 237

^a Previous literature results are included for comparison. ^b Drake, Standard, and Quandt.⁹ ^c This work.

represent the core 1s electrons of carbon and fluorine in Basis3 compared to an effective core potential in the SBKJC(3df) basis set.

B. Excited-State Results. Results obtained for the equilibrium geometry of the first excited singlet state of CFI, $\tilde{A}(^1A'')$, obtained using the CASPT2(18,12) method are reported in Table 2. The only previous computational results⁹ for the excited state are also presented. No experimental data is available for comparison.

As was discussed previously,⁹ no minimum could be located on the $\tilde{A}(^1A'')$ surface using lower levels of theory such as CASSCF(18,12) or CASPT2(2,2). In addition, even at the CASPT2(18,12) level, the equilibrium geometry of the CFI excited state exhibits extreme sensitivity to the basis sets employed in this study and in previous work.⁹ The C–I bond distance is particularly sensitive to the basis set; the equilibrium value varies by 0.3 Å, ranging from 2.13 to 2.43 Å. This large variation in the equilibrium C–I bond distance is in part due to the flat nature of the excited-state potential energy surface in the region of the minimum. For example, using the SBKJC(3d) basis set, varying the C–I distance from 2.15 to 2.45 Å with the C–F distance and F–C–I angle fixed at their equilibrium values leads to a change in energy of only 350 cm^{−1}. For the SBKJC(3df) basis set, a similar variation in the C–I distance leads to an energy change of only 250 cm^{−1}. These results show that on the excited-state surface, a slight change in the shape of the potential in the region of the minimum due to basis set effects may lead to a large shift in the equilibrium C–I bond distance.

Fluorocarbenes such as CFCl and CFBr show a small contraction of the equilibrium C–Cl or C–Br bond distance in the excited state relative to the ground-state equilibrium value. This is a well-known feature of halocarbenes and has been discussed in detail previously.⁹ The contraction of the C–Cl or C–Br bond distance in the excited-state arises because in the ground $\tilde{X}(^1A')$ state the nonbonding electrons on the carbon atom are located in an orbital that is coplanar with the C–F and C–X (X = Cl or Br) bonds. Excitation to the $\tilde{A}(^1A'')$ state places one of the nonbonding electrons in an orbital that is in a perpendicular orientation to the plane of the C–F and C–X bonds, allowing the F–C–X angle to increase relative to the ground-state value. The opening of the F–C–X angle leads to a slight reduction in the C–X bond length in the excited state. For example, in CFCl, calculations at the CASPT2(18,12)/cc-pVTZ level by Sendt et al.³ indicate that the excited-state C–Cl bond contracts by 0.06 Å relative to the ground-state value. For CFBr, CASPT2(18,12)/cc-pVTZ calculations by Kable and co-workers⁴ find a contraction of the C–Br bond of 0.03 Å in the

excited state. In contrast, for calculations of CFI using the SBKJC(3d) basis,⁹ the equilibrium excited-state C–I bond distance exhibits a large increase of 0.21 Å relative to the ground-state equilibrium bond distance. On the other hand, for calculations performed in this work employing the SBKJC(3df) basis and Basis3, contractions of 0.04 and 0.09 Å are obtained for the excited-state C–I bond distance relative to the ground-state values, respectively. On the basis of the contraction of the C–X bond observed in the excited-state geometries of CFCl and CFBr, our present results suggest that basis sets SBKJC(3df) and Basis3 better describe some aspects of the first excited singlet state of CFI than does the SBKJC(3d) basis set.

As was observed for the ground state, results obtained for the equilibrium geometry of the CFI $\tilde{A}(^1A'')$ excited state using the all-electron DZ(3df) basis set for carbon and fluorine in Basis3 are very similar to those obtained using the SBKJC(3df) basis set. Using Basis3, the equilibrium C–F bond is slightly shorter by 0.007 Å, the C–I bond is shorter by 0.035 Å, and the F–C–I angle is larger by 1.0° than the results obtained using SBKJC(3df) basis set.

C. Adiabatic Transition Energies. Electronic energies of the ground $\tilde{X}(^1A')$ and excited $\tilde{A}(^1A'')$ states of CFI are listed in Table 3, along with adiabatic transition energies (T_e) for the $\tilde{A}(^1A'') \leftarrow \tilde{X}(^1A')$ transition. Results from a previous literature study⁹ are also included. The calculated adiabatic transition energies for CFI range from 16237 to 17508 cm^{−1}.

While no experimental value of the $\tilde{A}(^1A'') \leftarrow \tilde{X}(^1A')$ transition energy is available for CFI, comparisons can be made with experiment for other halocarbenes such as CFBr. At the CASPT2(18,12)/SBKJC(3d) level, the calculated value of T_e for CFBr was 21369 cm^{−1},⁹ slightly higher but in excellent agreement with the experimental value of 20955 cm^{−1}.⁴ Note that the experimental value of T_{00} (20906 cm^{−1}) was adjusted using experimental vibrational zero-point energies⁴ to obtain the experimental value of T_e for comparison. When f-type polarization functions are included in the SBKJC(3df) basis set for CFBr, the transition energy is determined to be 19293 cm^{−1},¹⁸ slightly lower than the experimental result but again in reasonable agreement. Finally, when Basis3 is employed, the calculated transition energy for CFBr is 18031 cm^{−1},¹⁸ considerably lower than the experimental result. On the basis of the CFBr results, our best estimate for CFI is that the adiabatic transition energy lies between the values calculated using the SBKJC(3d) and SBKJC(3df) basis sets, or in the range 16960–17510 cm^{−1}. The result of 16240 cm^{−1} calculated using Basis3 probably underestimates the transition energy.

D. Details of the Excited-State Potential Surface. Because of the sensitivity of the equilibrium geometry of the CFI $\tilde{A}(^1A'')$

TABLE 4: Equilibrium Geometry and Electronic Energy of the Transition State on the Excited $\tilde{A}(^1A'')$ Potential Energy Surface of CFI^a

	CASPT2(18,12)/SBKJC(3d)	CASPT2(18,12)/SBKJC(3df)	CASPT2(18,12)/Basis3
C–F distance (Å)	1.300	1.292	1.283
C–I distance (Å)	2.557	2.531	2.522
F–C–I angle (deg.)	121.4	120.7	120.5
electronic energy (au)	−40.833597	−40.902097	−148.877087
barrier height (cm ^{−1})	475	1043	1525

^a Also reported is the height of the barrier to dissociation to CF + I, measured from the bottom of the potential well to the top of the barrier.

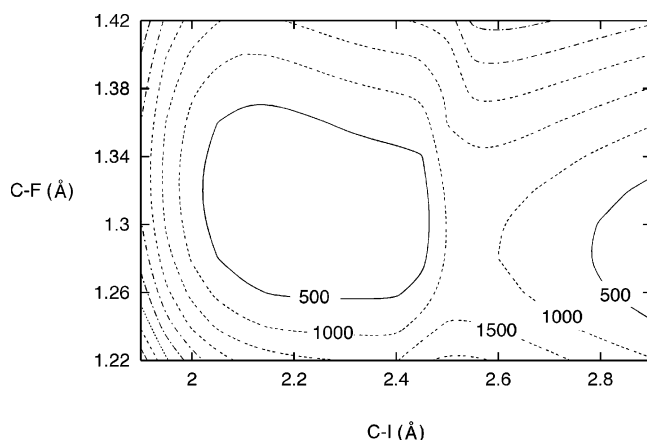


Figure 1. Contours of the CFI $\tilde{A}(^1A'')$ excited-state potential energy surface calculated at the CASPT2(18,12)/SBKJC(3df) level. The F–C–I angle was fixed at its equilibrium value of 124.8°. The energy contours in wavenumbers are measured from the bottom of the potential well.

excited state to the level of theory and basis set, the potential energy surface (PES) was mapped out at the CASPT2(18,12) level for selected basis sets. Figure 1 shows the dependence of the CFI excited-state PES on the C–F and C–I distances. In these calculations, single point energies were computed for selected C–F and C–I distances with the F–C–I bond angle fixed at its equilibrium value. The CASPT2(18,12)/SBKJC(3df) method was used to determine 231 points on the CFI excited-state PES in the range shown in Figure 1.

The most interesting features on the excited state PES are the shallow well followed by a gradual slope down to the dissociation products CF + I, producing a barrier due to an avoided crossing in the exit channel to dissociation. The barrier to dissociation can be characterized qualitatively by viewing a cut of the PES for fixed C–F distance in which the C–I bond distance is varied. Shown in Figure 2 are cuts along the CFI excited-state surface at the CASPT2(18,12)/SBKJC(3df) level of theory (a cut of the ground electronic state surface is also shown for comparison). In Figure 2, the C–F bond distance and the F–C–I bond angle are fixed at their equilibrium values for the excited state, while the C–I distance is varied from 1.7 to 6.0 Å. The cut along the excited-state potential in Figure 2 indicates that a barrier to dissociation occurs at a C–I distance of about 2.5 Å.

Starting with the approximate geometry for the barrier found in Figure 2, we carried out a transition state optimization. The optimized geometry of the transition state was determined using the CASPT2(18,12) method, and the results are summarized in Table 4. The optimized geometrical parameters of the transition state are similar when computed using the three different basis sets. The equilibrium C–I bond distance for the transition state is more elongated when computed with the SBKJC(3d) basis, 2.56 Å compared to 2.52–2.53 Å for the other basis sets. The calculated barrier height, measured from the bottom of the

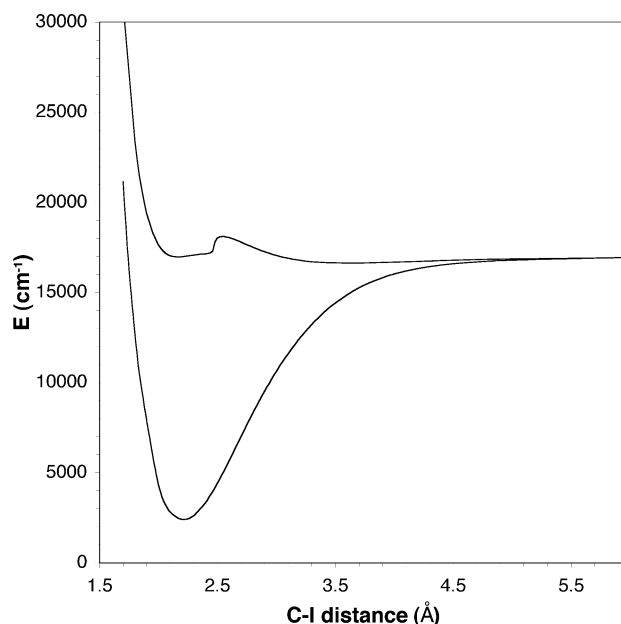


Figure 2. Cut through the CFI $\tilde{A}(^1A'')$ excited-state potential energy surface along the C–I bond calculated at the CASPT2(18,12)/SBKJC(3df) level. The C–F bond distance and the F–C–I bond angle were fixed at their equilibrium values. Also shown for comparison is a similar cut through the CFI $\tilde{X}(^1A')$ ground-state surface, with the C–F bond distance and F–C–I bond angle fixed at the equilibrium values for the excited state. Energies in wavenumbers are measured from the minimum on the ground-state potential energy surface.

excited-state potential well to the top of the barrier, ranges from 475 to 1525 cm^{−1} depending on the basis set.

The basis set dependence of the dissociation barrier can be explored by examining results from similar calculations for CFBr. The dissociation barrier of CFBr was determined using the CASPT2(18,12) method to be 953, 2150, and 2776 cm^{−1} for the basis sets SBKJC(3d), SBKJC(3df), and Basis3, respectively.¹⁸ The CFBr dissociation barrier results show a pattern similar to the results reported in this work for CFI. The experimental barrier to dissociation for CFBr is 3360 ± 50 cm^{−1},⁵ about 580 cm^{−1} larger than the result obtained using Basis3 and significantly larger than the other two values determined using the SBKJC(3d) and SBKJC(3df) basis sets. Assuming a similar basis set dependence, the experimental dissociation barrier of CFI probably lies above our largest calculated value of 1525 cm^{−1}.

The structure of the CFI $\tilde{A}(^1A'')$ PES is similar to those previously determined for CFBr and CFCI. For CFBr, a barrier height of 3455 cm^{−1} was calculated at the CASPT2(18,12)/cc-pVTZ level⁴ compared to an experimental value of 3360 ± 50 cm^{−1}.⁵ For CFCI, the barrier to dissociation was determined to be 5699 cm^{−1} at the CASPT2(18,12)/cc-pVTZ level,³ compared to the experimental result of 4073 cm^{−1}.² Note that the literature results give vibrational zero-point corrected barrier heights while the results reported in this work have not been corrected for vibrational zero-point energies. On the basis of the results for

CFCl and CFBr, it appears that the present CASPT2(18,12) results for CFI are in accord with the type of dissociation barrier expected for these systems. In addition, the barrier height of greater than 1525 cm^{-1} predicted for CFI fits a trend of decreasing barrier heights in the series $\text{CFCl} > \text{CFBr} > \text{CFI}$.

4. Conclusions

Equilibrium geometries for the ground $\tilde{X}(^1A')$ and excited $\tilde{A}(^1A'')$ electronic states of CFI as well as adiabatic transition energies have been obtained using the CASPT2(18,12) method. Three different basis sets were employed to investigate the sensitivity of the results to the basis set. Results for the ground-state equilibrium geometry of CFI are in excellent agreement with previous studies.⁷⁻⁹ The equilibrium geometry of the first excited singlet state of CFI, determined using basis sets containing f-type polarization functions, shows a slight contraction of the C-I bond relative to the ground-state value. These results are in agreement with the behavior observed in previous experimental and computational studies of CFCl ^{2,3} and CFBr .^{4,5}

The $\tilde{A}(^1A'') \leftarrow \tilde{X}(^1A')$ adiabatic transition energy for CFI is believed to lie between 17000 and 17500 cm^{-1} based on comparisons between calculation and experiment for other fluorocarbenes. A transition state with a C-I bond distance of about 2.5 \AA has also been located on the $\tilde{A}(^1A'')$ excited-state surface in the exit channel for dissociation to $\text{CF} + \text{I}$. The calculated barrier height on the $\tilde{A}(^1A'')$ surface is estimated to be greater than 1525 cm^{-1} using the CASPT2(18,12) method. While no experimental data is available on CFI for comparison, the calculated barrier is in accord with those known for CFBr and CFCl . These new more accurate predictions of the properties of the ground and first excited singlet states of CFI as well as the $\tilde{A}(^1A'') \leftarrow \tilde{X}(^1A')$ adiabatic transition energy should provide useful information for further experimental investigations of this interesting halocarbene.

Acknowledgment is made to the Illinois State University Research Grant program and to the National Center for Supercomputing Applications for partial support of this work.

References and Notes

- (1) Karolczak, J.; Joo, D. L.; Clouthier, D. J. *J. Chem. Phys.* **1993**, *99*, 1447.
- (2) Guss, J. S.; Votava, O.; Kable, S. H. *J. Chem. Phys.* **2001**, *115*, 11118.
- (3) Sendt, K.; Schmidt, T. W.; Bacskay, G. B. *Int. J. Quantum Chem.* **2000**, *76*, 297.
- (4) Knepp, P. T.; Scalley, C. K.; Bacskay, G. B.; Kable, S. H. *J. Chem. Phys.* **1998**, *109*, 2220.
- (5) Knepp, P. T.; Kable, S. H. *J. Chem. Phys.* **1999**, *110*, 11789.
- (6) Carter, E. A.; Goddard, W. A. *J. Chem. Phys.* **1988**, *88*, 1752.
- (7) Hajgato, B.; Nguyen, H. M. T.; Veszpremi, T.; Nguyen, M. T. *Phys. Chem. Chem. Phys.* **2000**, *2*, 5041.
- (8) Schwartz, M.; Marshall, P. *J. Phys. Chem. A* **1999**, *103*, 7900.
- (9) Drake, S. A.; Standard, J. M.; Quandt, R. W. *J. Phys. Chem. A* **2002**, *106*, 1357.
- (10) Sendt, D.; Bacskay, G. B. *J. Chem. Phys.* **2000**, *112*, 2227.
- (11) Karolczak, J.; Clouthier, D. J. *J. Chem. Phys.* **1991**, *94*, 1.
- (12) Scherer, J. J.; Paul, J. B.; O'Keefe, A.; Saykally, R. J. *Chem. Rev.* **1997**, *97*, 25.
- (13) Min, Z.; Wong, T.-H.; Quandt, R.; Bersohn, R. *J. Phys. Chem. A* **1999**, *103*, 10451.
- (14) MOLPRO is package of ab initio programs designed by H.-J. Werner and, P. J. Knowles, version 2002.3. Amos, R. D.; Bernhardsson, A.; Berning, A.; Celani, P.; Cooper, D. L.; Deegan, M. J. O.; Dobbyn, A. J.; Eckert, F.; Hampel, C.; Hetzer, G.; Knowles, P. J.; Korona, T.; Lindh, R.; Lloyd, A. W.; McNicholas, S. J.; Manby, F. R.; Meyer, W.; Mura, M. E.; Nicklass, A.; Palmieri, P.; Pitzer, R.; Rauhut, G.; Schütz, M.; Schumann, U.; Stoll, H.; Stone, A. J.; Tarroni, R.; Thorsteinsson, T.; Werner, H.-J.
- (15) Stevens, W. J.; Basch, H.; Krauss, M. *J. Chem. Phys.* **1984**, *81*, 6026.
- (16) Stevens, W. J.; Basch, H.; Krauss, M.; Jasien, P. *Can. J. Chem.* **1992**, *70*, 612.
- (17) Cundari, T. R.; Stevens, W. J. *J. Chem. Phys.* **1993**, *98*, 5555.
- (18) Standard, J. M.; Quandt, R. W. Unpublished results.